Multivalued distributions of electrons between equivalent valleys of silicon in a magnetic field

M. Asche, V. M. Ivashchenko, H. Kostial, and V. V. Mitin

Central Institute of Electron Physics, Academy of Sciences of the German Democratic Republic, Berlin, East Germany
Institute of Semiconductors, Academy of Sciences of the Ukrainian SSR, Kiev

(Submitted January 23, 1984; accepted for publication May 25, 1984)

Fiz. Tekh. Poluprovodn. **18**, 1660–1667 (September 1984)

Multivalued distributions of electrons between three equivalent valleys in *n*-type Si subjected to a magnetic field are considered in the case when the direction of flow of the current is rotated slightly away from [111] toward [110]. Experimental and numerical evidence is given for the first time that multivalued electron distributions appear near theoretically predicted loop-like sections of the current-voltage characteristics. Such sections appear in the absence of a magnetic field for the currents flowing along the [111] direction; in the presence of a magnetic field when the total (Hall and longitudinal) electric field heats identically all three pairs of valleys these multivalued distributions give rise to strong electric fields transverse to the current and the dependences of the current on the magnetic field then exhibit abrupt changes of the current.

1. Multivalued electron distributions between valleys in n-type Si had been discovered earlier[1] and investigated in detail at low temperatures for the current **j** along the [110] direction,[2] and later in a wide range of directions of **j** in a ($\bar{1}10$) plane between the [110] and [111] axes.[3] These multivalued distributions are manifested as follows: instead of a homogeneous distribution with equal populations of two valleys located symmetrically relative to the current, a sample splits into layers parallel to the current and one of the valleys is then occupied preferentially in a given layer. The number of layers and their sequence are governed by the conditions on the side surfaces of a sample and by its inhomogeneities.[4,5]

When the direction of the flow of the current is close to [111], the third valley begins to affect the results and if $\mathbf{j} \parallel [111]$, then instead of the equal population of the three valleys, it is found that a multivalued electron distribution gives rise to stratification with a preferential occupancy of one of the valleys in each of the layers.[6] The existence of multivalued electron distributions for **j** close to the [$\bar{1}\bar{1}1$] direction was demonstrated experimentally in Ref. 7.

We shall report an investigation of multivalued electron distributions for small deviations of the direction of the current from [111] toward [110] and we shall concentrate our attention on the effects of a magnetic field transverse to the current on such distributions.

2. Our samples were prepared from n-type Si with a donor concentration of $N_D = 5 \cdot 10^{13}$ cm^{-3} and an acceptor concentration $N_A = 5 \cdot 10^{12}$ cm^{-3}. We employed samples of shape shown in Fig. 1, which gives also the orientations of the crystallographic and coordinate axes on the side faces, and the projections of the valleys on the end surfaces which carried contacts 1 and 2. The deviation of the x axis from the [111] direction and, consequently, of the two side faces from ($11\bar{2}$) planes was ~ 6–7°. The other two side faces coincided with ($\bar{1}10$) planes. The angle φ was the deviation of the magnetic field **H**, applied in the yz plane, from the [$\bar{1}\bar{1}0$] axis; this angle was measured so that for $\varphi = 0$ the total electric field E deviated from the x axis toward [111] because of the appearance of the Hall field E_H, whereas $\varphi = 90°$ the Hall field was $E_{H\parallel}$ [$\bar{1}10$]. Measurements were made in liquid neon (27.1 K).

In calculations of the effects occurring in the range of existence of multivalued electron distributions in silicon subjected to a magnetic field it is necessary to solve a system of transcendental equations for the transverse fields E_x and E_y (see the Appendix), obtained by equating to zero the transverse currents, and then determine the total current j. These transcendental equations include quantities that depend on the effective fields E_α and H_α in a valley α (this is explained later), such as $\nu_\parallel$ (E_α, H_α) and $\nu_\perp$ (E_α, H_α) representing the drift velocities of electrons in a valley α directed along E_α and [$E_\alpha \cdot H_\alpha$], respectively, as well as $\tau(E_\alpha, H_\alpha)$ representing the time for the transfer of electrons from a valley α to one of the other valleys designated by $\gamma \neq \alpha$. These dependences on E_α and H_α are found employing numerical modeling of the transport processes in n-type Si by the Monte Carlo method.

The procedure for the calculation in the H = 0 case was described in Refs. 2, 3, and 6. In the present study we used the same values of the electron–phonon interaction constants and assumed that the intervalley impurity scattering time τ_0 is 10^{-7} sec (Ref. 3). The application of a magnetic field has the effect that for each of the valleys α we must introduce not only an effective electric field E_α [$E_j^{(\alpha)} = \beta_j E_j$, where E_j are the projections of the total electric field along the axis of a valley; if the axis 3 is directed along the axis of revolution of a constant-energy ellipsoid, then $\beta_{1,2} = \sqrt{m_\perp/m}$, $\beta_3 = \sqrt{m_\parallel/m}$, where $m = (m_\perp^2 m_\parallel)^{1/3}$, $m_\parallel$ and $m_\perp$ are the longitudinal and transverse effective masses[2,3,6]], but also an effective magnetic field[8] denoted by H_α ($H_{1,2}^{(\alpha)} = \beta_1\beta_3 H_{1,2}$; $H_3^{(\alpha)} = \beta_1^2 H_3$).

Figure 2 shows the results of calculations of the dependences of the drift velocities $v_\parallel$ and $v_\perp$ and of the reciprocal scattering times τ^{-1} on E_α (with H_α as a parameter) calculated for 27 K on the assumption of the interaction with intervalley f_1 (0.018 eV) and f_2 (0.047 eV) phonons. We can see that the dependences of $v_\parallel$ and τ^{-1} on H become significant only in fields $H_\alpha > 1$ kOe. Since all the characteristic features in the case of small deviations from the [111] direction were observed in fields $H_\alpha < 1$

 0038-5700/84/09 1038-05 $03.90

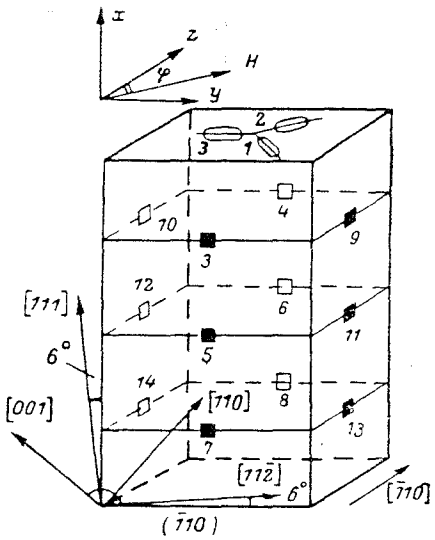

FIG. 1. Schematic representation of the shape of a sample, orientations of the coordinate axes relative to the faces of the sample, positions of the measuring probes on the side faces, and projections of the valleys on the end surfaces.

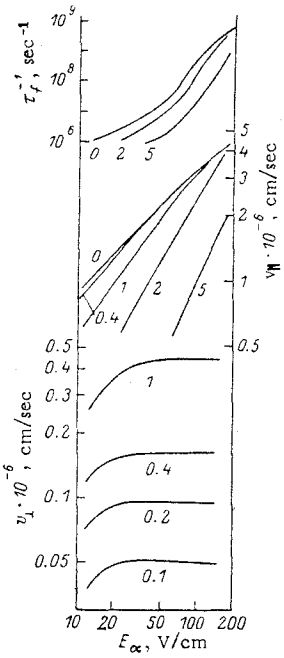

FIG. 2. Results of Monte Carlo calculations of the drift velocities $v_\parallel \parallel \mathbf{E}_\alpha$ and $v_\perp \parallel [\mathbf{E}_\alpha \cdot \mathbf{H}_\alpha]$ and of the reciprocal transfer time τ_f^{-1} from a valley α as a function of the electric field E_α in the valley α, plotted for different values of H_α. The numbers alongside the curves are the fields H in kilo-oersted.

kOe, we carried out calculations on the assumption that $\nu_\parallel(E_\alpha)$ and $\tau^{-1}(E_\alpha)$ were independent of H_α and we allowed only for the dependence of $\nu_\perp(E_\alpha)$ on H_α. In this approximation we can consider any mutual orientation of E and H, and not only $E \perp H$.

3. Figure 3a shows the current-voltage characteristics determined under static conditions for different values and directions of H. If $H = 0$, then in moderate electric fields $E_X = u/l$ (l is the length of the sample and u is the applied voltage) ranging from 51 to ≈ 82 V/cm there is a current-saturation region. This region is observed because the current-voltage characteristic calculated on the assumption of a homogeneous distribution of the field E and of the current j (Fig. 3b) has an N-type negative differential conductance (N-NDC) region. This region is observed because, instead of equal occupany of the valleys 1 and 2 located symmetrically relative to the current, one of the valleys is occupied preferentially so that a multivalued electron distribution is established.[3] Domains appear because of the instability of this part of the current-voltage characteristic. If a high-field domain appears at the anode and broadens on increase in the voltage toward the cathode, the saturation current coincides

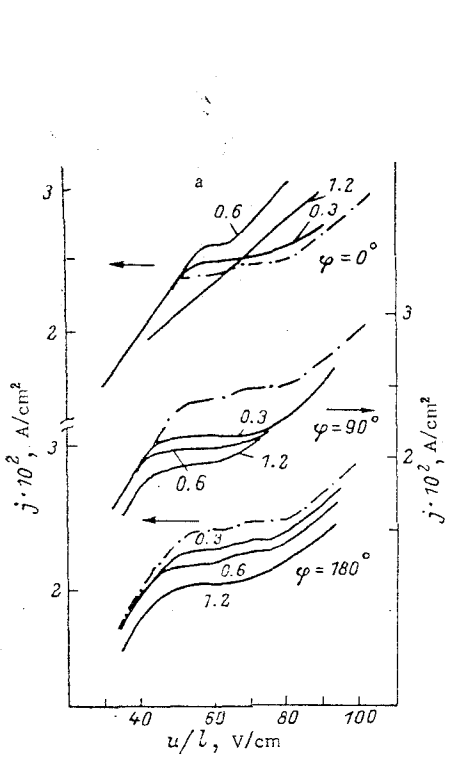

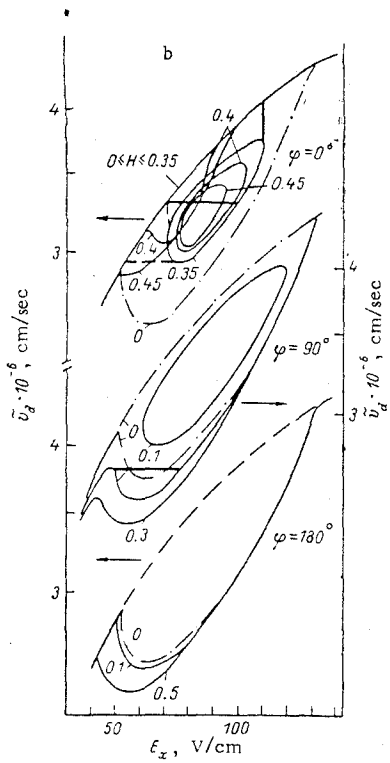

FIG. 3. Current-voltage characteristics obtained for different values and directions of H: a) measured under static conditions; b) calculated. The numbers alongside the curves give the fields H in kilo-oersted.

with the maximum of the current-voltage characteristic (see the Appendix 2 in Ref. 9), as indicated by the thicker curve in Fig. 3b for $\varphi = 90°$, in agreement with the experimental results.

The current-voltage characteristics are the same for the angles $\varphi = 90$ and 270° because reversal of the magnetic field direction reverses the Hall field oriented along the $[\bar{1}10]$ symmetry axis. The current-saturation region becomes narrower on increase in H and the value of the saturation current decreases, in agreement with the calculations (Fig. 3b); this is due to rotation of the total field E from the xy plane in the direction of the axis of the valleys 1 or 2, depending on the polarity of H, and by the consequent increase in the effective heating field in the valley 2 or 1, respectively.

Similar changes in the current-voltage characteristics on increase in the magnetic field intensity are also observed for $\varphi = 180°$, but in this case the Hall field does not disturb the symmetric configuration of the valleys 1 and 2 relative to the total field E in the absence of a multivalued electron distribution, but simply rotates this configuration toward the [110] axis. Such multivalued electron distributions are observed in a magnetic field.

A completely different situation is encountered for $\varphi = 0$. In this case an increase in H first causes rapid narrowing of the saturation region accompanied by a simultaneous increase in the saturation current, and then the current-voltage characteristic assumes the same form as that of the characteristic obtained in H = 0 for $\mathbf{j} \parallel [111]$ and the current decreases. It is clear from the current-voltage characteristics calculated for the homogeneous case (Fig. 3b) that in the case when H = 0 or when H is low there is an N-NDC region, as described earlier for the other orientations of H. In a field H = 0.2 kOe a loop-shaped section splits off from the branch of

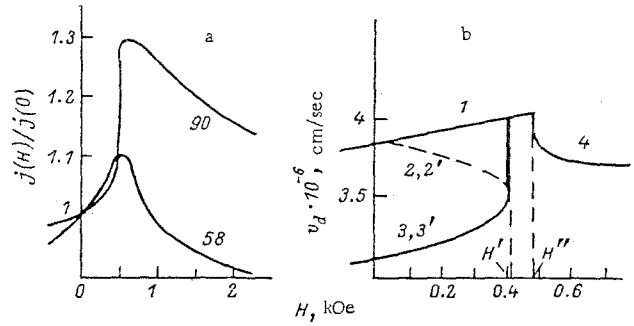

FIG. 4. Dependences of the current on the magnetic field for $\varphi = 0$: a) measured (in fields E_x, expressed in volts per centimeter and given alongside each curve); b) calculated (for $E_x = 90$ V/cm).

the current-voltage characteristic corresponding to the equal populations of the valleys 1 and 2 and this section corresponds to a preferential occupancy of one of the valleys 1 or 2. On increase in H the loop becomes narrower and it disappears in H = 0.6 kOe. A comparison with the experimental results confirms the existence of loop sections if a transition takes place in the saturation region, as indicated by a thicker continuous curve, but no transition takes place on reduction of the current, as indicated by a thicker dashed curve in Fig. 3b.

Figure 4a shows the magnetic-field dependences of the current for two values of E_x: the first (58 V/cm) corresponds to the current-saturation region, whereas the second (90 V/cm) is outside the region where the distribution of the field E_x is already homogeneous and we can compare the results with the calculated dependences. If a two-layer distribution with equal dimensions of the layers is established in a sample when H = 0, then for $\varphi = 90°$ (H > 0) and $\varphi = 270°$ (H < 0) an increase in H shifts the wall separating the layer with a preferential

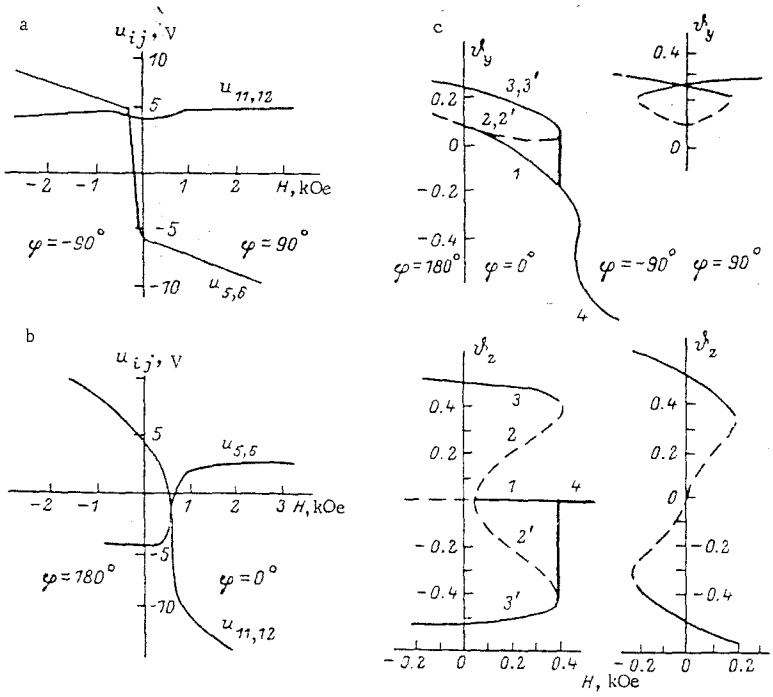

FIG. 5. a, b) Measured potential differences u_{ij} between the probes of a sample (Fig. 1). c) Dependences of the transverse fields $\vartheta_y = E_y/E_x$ and $\vartheta_z = E_z/E_x$ on the magnetic field calculated for different values of φ.

occupancy of the valley 1 from the layer with a preferential occupany of the valley 2; the shift is toward one of the side surfaces and the current j(H) is not affected by a reversal of H but decreases for both directions of the magnetic field as H is increased in accordance with the theory. However, the experimental results are different: a practically single-layer distribution is observed for this sample in $H = 0$ and it is characterized by a preferential occupancy of the valley 1, which can be seen clearly in Figs. 5a and 5b where we have plotted the measured potential differences between probes 5 and 6, 11 and 12, and 5 and 12 as a function of H together with the calculated transverse fields $E_y(H)$ and $E_z(H)$ (Fig. 5c). The position of the interlayer wall in the middle of the sample corresponds to $u_{5,6} = 0$. Variation of H for $\varphi = 90°$ leaves $u_{11,12}$ practically unchanged, whereas $U_{5,6}$ undergoes a sudden almost jump-like change, which corresponds to a shift of the interlayer wall along the z axis from one side face to the other (Fig. 5a). The maximum value of the current in Fig. 4 corresponds to the position of the interlayer wall at the center of the sample. The fall of the current near the maximum is influenced by the contact regions because the average field in the sample is given by $\overline{E_x} = u/l$. Multivalued electron distributions observed at $H = 0$ give rise to a large transverse field (which in our case exceeds 50 V/cm). This field is short-circuited by the current contacts so that a transition region of the order of the crystal size d forms along the transverse field, whereas for the central position of the interlayer wall the size of this region is of the order of d/2.

If $\varphi = 0$, then an increase in H gives rise to a sudden almost jump-like increase in the current in the vicinity of $H = 0.6$ kOe (Fig. 4a) and it causes abrupt changes in the transverse fields (Figs. 5b and 5c).

In the region of abrupt changes in j and u_{ij} the calculated dependences show transitions between the various branches of the solutions, whereas an abrupt change in the current corresponds to a thicker continuous line in Figs. 4b and 5c, which is due to the appearance and rapid spreading to the whole of the sample (on increase in H) of a high-current layer with its boundaries parallel to the current. A preferential occupancy of the valley 3 occurs in this layer so that the sign of $u_{11,12}$ is reversed, whereas $u_{5,6}$ does not vanish only because the probe 6 is not located at the point opposite to probe 5 so that the fields E_y and E_x do contribute to $u_{5,6}$.

Figure 6a shows the experimental dependence of the current on the angle of rotation of the magnetic field in the yz plane. The angular range $\varphi = 180$-$360°$ is a mirror image of the range $\varphi = 180$-$0°$. According to the dependences calculated for low fields $H < 0.1$ kOe (Fig. 6b), we can have two values of the current for $\varphi = 0$ and 180°: the upper value corresponds to equal occupancies of the valleys 1 and 2 (which is unstable because of a multivalued electron distribution), whereas the lower is doubly degenerate and corresponds to a preferential occupancy of the valley 1 or the valley 2. If $0 < \varphi < 180°$, then the degeneracy is lifted and both solutions are stable also for a homogeneous distribution of electrons. Since in the case of a multivalued electron distribution a homogeneous sample splits in $H = 0$ into no more than two layers (one with a preferential occupancy of the valley 1 and the other of the valley 2) and the interlayer wall separating them shifts rapidly on increase in H ($\varphi = 90°$), so that the sample becomes effectively single-layer,[2,4,6] the experimental results correspond to the current represented by the lower thicker line. An increase in H causes merging of the two upper solutions, so that for φ near 70° there is only one solution (as indicated by the current-voltage characteristic plotted in Fig. 3b for $\varphi = 90°$). When $\varphi = 0$, an increase in H corresponds to a deviation of the total field E toward [111] and in a certain field $H = H_c$ we find (Figs. 4b and 5c) that solutions corresponding to a slight preferential occupancy of the valley 1 or the valley 2 split off from a solution corresponding to an equal occupancy of the two valleys (curve 1). Curves 2 and 2' correspond to the same current and are unstable, whereas a solution with an equal occupancy of the valleys 1 and 2 becomes stable and corresponds to the maximum current. If $\varphi > 0$, then the degeneracy of the solutions with preferential occupancies of the valleys 1 and 2 is lifted and therefore the dependence $j(\varphi)$ exhibits a second loop, as demonstrated in Fig. 6b (cases II and III). The dependence $j(\varphi)$ is extended to the range of angles $\varphi < 0$ in order to demonstrate that the solution corresponding to a preferential occupancy of one valley is continuous and S-shaped.

The appearance of a new stable solution is not reflected in the experimental dependences because the minimum value of the current corresponding to the maximum transfer of electrons to either the valley 1 or the valley 2 (curves 3 and 3' in Figs. 4b and 5c). An increase in H widens the range of existence of a solution with equal populations of the two valleys (Fig. 6b) and the current j corresponding to the stable region is practically unaffected up to $H \approx 0.45$ kOe.

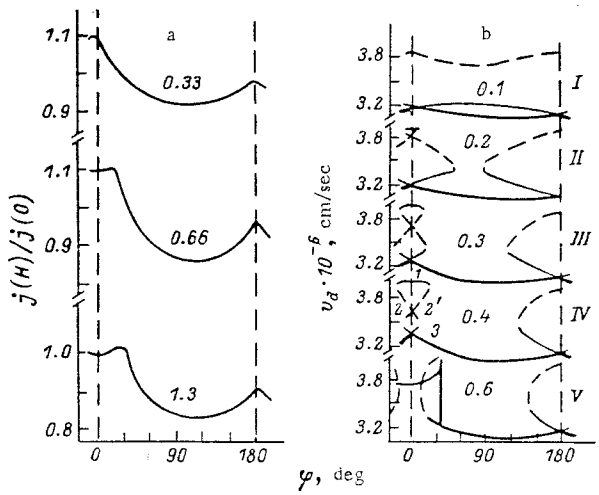

FIG. 6. Dependences of the current on the angle of rotation of the magnetic field in the xy plane of a sample subjected to $E_x = 100$ V/cm: a) measured dependences; b) calculated results. The numbers alongside the curves give the fields H in kilo-oersted. In case IV the various types of solutions corresponding to analogous curves in Figs. 4b and 5c are designated by 1, 2, 2', and 3, and they correspond to analogous curves in Figs. 4b and 5c.

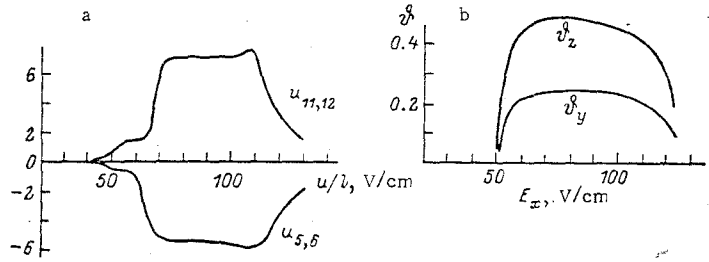

FIG. 7. Dependences of the measured potential difference u_{ij} (a) and of the calculated transverse fields (b) on the applied electric field in the case when H = 0.

If H > H' then for a certain angle φ a transition takes place between solutions of types 1 and 3 and this occurs along a practically vertical line corresponding (as before) to the appearance of a high-current layer when a multivalued electron distribution between the valleys 1 and 2 disappears and the layer becomes broader on reduction in φ. Finally, if H = H'' then a solution with a preferential occupancy of the valley 3 appears for $\varphi = 0$ (curves denoted by 4 in Figs. 4b and 5c) and the current decreases. If H > H'', then the dependence $j(\varphi)$ exhibits a loop (case V in Fig. 6b), the current corresponding to $\varphi = 0$ decreases, and the transition from small to large currents shifts toward ever-increasing values of φ. One should point out particularly that the presence of a loop in the case of the dependence $j(\varphi)$ observed in fields H > 0.5 kOe is due to an accidential equality of the currents for different values of the transverse field $E_\perp$, because $E_\perp(H)$ has the usual S-shaped form with an unstable middle solution, which makes it possible to identify the unstable branch represented by dashed curves in case IV. In Figs. 4b, 5c, and 6b a selected value of the electric field is such that H'' > H' (H'' increases on increase in E_X, whereas H' decreases, as shown in Fig. 3b). In the case of electric fields E_X such that H'' < H', the transition from solutions of type 3 and 3' to those of type 4 occurs in H = H''.

It is worth noting that if $\varphi = 30°$ then both the experimental and calculated values of the current are practically independent of the magnetic field since this field creates a Hall electric field perpendicular to the anisotropic field of a multivalued electron distribution and if H is small, then the change in the latter is slight.

We shall conclude by noting that the range of external electric fields corresponding to the appearance of multivalued electron distributions is 48-120 V/cm, which is demonstrated in Fig. 7 showing the dependence of the potential differences $u_{5,6}$ and $u_{11,12}$ and of $\vartheta_{y,z}$ on the electric field E_X applied in the case when H = 0.

APPENDIX

The expressions for the x, y, and z components of the current in a sample with the orientations of the crystallographic axes relative to the coordinate axes shown in Fig. 1 are as follows

$$j_x(E) = \frac{nE_x}{\tau_\Sigma}\{F_{1x} + aF_{2x}(1 - 3\cos 2\psi) + \vartheta_y[-3a\sin 2\psi F_{2x} - 2a\sin\psi F_{3y} + F_{1x}(1 - 2a) - 6aZ_3] + \vartheta_z[3a\cos 2\psi F_{2y} - 6a\sin\psi F_{3x} - F_{1y}(1 - 5a) - 3aY_3 + 6a\cos\psi F_{3x}]\}, \quad \text{(A.1a)}$$

$$j_y(E) = \frac{nE_x}{\tau_\Sigma}\{-3a\sin 2\psi F_{2x} + 6a\sin\psi F_{3y} - F_{1x}(1 - 2a) + 6aZ_3 + \vartheta_y[F_{1x} + aF_{2x}(1 + 3\cos 2\psi)] + \vartheta_z[3a\sin 2\psi F_{2y} + 6a\sin\psi F_{3x} - 6a\cos\psi F_{3x}]\}, \quad \text{(A.1b)}$$

$$j_z(E) = \frac{nE_x}{\tau_\Sigma}\{-3a\cos 2\psi F_{2y} + 6a\sin\psi E_{3x} + F_{1y}(1 - 5a) + 3aY_3 - 6a\sin\psi F_{3x} + \vartheta_y[-3a\sin 2\psi F_{2y} + 6a\sin\psi F_{3x} + 6a\cos\psi F_{3x}] + \vartheta_z[F_{1x} - 2aF_{2x}]\}, \quad \text{(A.1c)}$$

where

$$F_{1j} = J_1 + J_2 + J_3, \quad X_i = v_\parallel(E_i)\tau(E_i)/E_i,$$
$$F_{2j} = J_1 + J_2 - 2J_3, \quad Y_i = \chi H_y v_\perp(E_i)\tau(E_i)/E_i,$$
$$F_{3j} = J_1 - J_2, \quad Z_i = \chi H_x v_\perp(E_i)\tau(E_i)/E_i,$$
$$J_i = X_i, Y_i, Z_i, \quad H_y = H\sin\varphi, \quad H_x = H\cos\varphi,$$
$$\tau_\Sigma = \tau(E_1) + \tau(E_2) + \tau(E_3), \quad \chi = (1 + 4a)\left(\frac{2m}{m_\perp} + \frac{m}{m_\parallel}\right)^2\Big/9,$$
$$a = \frac{1}{4}\frac{m_\parallel - m_\perp}{2m_\parallel + m_\perp},$$

and ψ is the angle between the [110] direction and the x axis.

The electric field components E_Y and E_Z corresponding to a given value of E_X can be calculated from

$$\begin{cases} j_y = 0, \\ j_z = 0. \end{cases}$$

Knowing E_Y and E_Z, we can use Eq. (A.1) to determine the current j_X for an arbitrary value of the magnetic field when H ⊥ E where E is the total electric field.

[1] M. Asche, H. Kostial, and O. G. Sarbei, J. Phys. C 13, L645 (1980).
[2] M. Asche, Z. S. Gribnikov, V. M. Ivashchenko, H. Kostial, V. V. Mitin, and O. G. Sarbei, Preprint [in Russian], Institute of Physics, Academy of Sciences of the Ukrainian SSR, Kiev (1981); Zh. Eksp. Teor. Fiz. 81, 1347 (1981) [Sov. Phys. JETP 54, 715 (1981)].
[3] M. Asche, Z. S. Gribnikov, V. M. Ivashchenko, H. Kostial, and V. V. Mitin, Phys. Status Solid B 114, 429 (1982).
[4] Z. S. Gribnikov and V. V. Mitin, Pis'ma Zh. Eksp. Teor. Fiz. 14, 272 (1971) [JETP Lett. 14, 182 (1971)]; Phys. Status Solidi B 68, 153 (1975).
[5] Z. S. Gribnikov, Zh. Eksp. Teor. Fiz. 83, 718 (1982) [Sov. Phys. JETP 56, 401 (1982)].
[6] M. Asche, Z. S. Gribnikov, V. V. Mitin, and O. G. Sarbei, Hot Electrons in Many-Valley Semiconductors [in Russian], Kiev (1982).
[7] M. Asche and H. Kostial, Phys. Status Solidi B 120, K83 (1983).
[8] V. M. Ivashchenko and V. V. Mitin, Ukr. Fiz. Zh. 29, 123 (1984).
[9] Z. S. Gribnikov, V. M. Ivashchenko, V. V. Mitin, and O. G. Sarbei, Preprint [in Russian], Institute of Physics, Academy of Sciences of the Ukrainian SSR, Kiev (1981).

Translated by A. Tybulewicz